

MINIMISING POWER LOAD ASYMMETRIES DURING DISRUPTION MITIGATION AT JET

S. JACHMICH

Laboratory for Plasma Physics, Ecole Royale Militaire/Koninklijke Militaire School, TEC partner
Av de la Renaissance 30, Brussels, Belgium
Email: stefan.jachmich@euro-fusion.org

M. LEHNEN

ITER Organization,
Route de Vinon sur Verdon, CS 90 046, 13067 Saint Paul-lez-Durance, France

P. DREWELow

Max-Planck Institut fuer Plasmaphysik
Greifswald, Germany

U. KRUEZI

ITER Organization
Route de Vinon sur Verdon, CS 90 046, 13067 Saint Paul-lez-Durance, France

I. S. CARVALHO

Inst. de Plasmas e Fusao Nuclear, Inst. Sup. Tecnico
Lisboa, Portugal

M. IMRISEK

IPP.CR
Prague, Czech Republic

V. PLYUSNIN

Inst. de Plasmas e Fusao Nuclear, Inst. Sup. Tecnico
Lisboa, Portugal

C. REUX

CEA, IRFM
St Paul Lez Durance, France

JET CONTRIBUTORS

See the author list of "X. Litaudon et al 2017 Nucl. Fusion 57 102001"
EUROfusion Consortium JET
Abingdon, United Kingdom

Abstract

The high thermal loads caused by a disruption of an ITER baseline scenario pulse with stored thermal energy of 350MJ and magnetic energy inside the vessel of 400 MJ pose a severe threat to the first wall components. Massive gas injection (MGI) into a disrupting plasma in JET has been shown to be capable of reducing the energy deposited onto the plasma facing components by increasing the radiation. However, the uneven distribution of the radiated power following a single local massive gas injection leads to highly localised radiation and hence to significant thermal loads due to the radiation "flash". In addition, the presence of the $n=1$ mode during the disruption produces toroidal and poloidal radiation asymmetries. In order to address this issue, JET has installed three MGI-valves. Single or a combination of two MGI-valves have been fired into a locked error field mode, whose toroidal O-point position was imposed by applying an external $n=1$ magnetic perturbation field. By measuring the radiated power at two separate toroidal locations and varying the toroidal phase of the perturbation field a toroidal peaking factor TPF, defined as the ratio of the maximum radiation to the average value, could be estimated. For a single injection TPFs in the range of 1.5 up to 1.8 have been found, depending on the type of impurity gas used. Optimising the time delay between two MGI-valves, which are toroidally at opposite locations, allowed a reduction of the TPF down to 1.2. This paper summarises the experimental findings of radiation asymmetries during mitigated disruptions caused by a seeded error field mode and compares the result with a heuristic model.

1. INTRODUCTION

During an unmitigated disruption of an ITER pulse, the stored thermal energy and the magnetic energy inside the vessel will be deposited onto the first wall or the divertor through conduction. This locally concentrated deposition can lead to surface melting already at energies well below the target energies of 350 MJ thermal and 400 MJ magnetic for the 15 MA baseline scenario [1]. The injection of massive amounts of high-Z gas aims on dissipating the energy through line radiation and by this distributing the thermal load over larger areas to prevent temperatures exceeding the melt limits. However, the distribution of the radiated power can be highly non-uniform due to the localised injection of the gas and due to the presence of MHD modes that drive the thermal quench. It was found that a single local massive gas injection (MGI) leads to highly localised radiation and hence to significant thermal loads to the first wall due to the radiation “flash” [2]. In addition, the presence of the $n=1$ mode during the disruption produces toroidal and poloidal radiation asymmetries as it has been shown by NIMROD calculations for DIII-D H-mode experiments [3, 4]. Depending on the phase relationship between the $n=1$ mode and the MGI-location, this effect can be enhanced or diminished.

The technique to inject massive amount of high-Z material for disruption mitigation in ITER will be Shattered Pellet Injection. This technique will deliver the gas more efficiently to the plasma in a device of this size. Presently, three toroidal injection positions are planned to inject a total of 32 pellets [M. Lehnen *et al.*, this conference]. The pellet fragments will have different characteristics in radial, poloidal and toroidal spreading compared to MGI. This behaviour will also depend strongly on the fragment sizes and the pellet velocity. However, the understanding of the dynamics of the thermal quench is still limited. This motivates the detailed analysis of the MGI experiments reported here. JET is soon commissioning its SPI injector and experiments are planned for the coming campaign. The comparison between MGI and SPI radiation distributions will aid improving the understanding of the underlying process and it will deliver important input for model validation.

The toroidal radiation asymmetry can be characterised by a toroidal peaking factor given by the ratio of the toroidal maximum radiated power to the average radiated power. In order to determine the toroidal peaking factor in disrupted mitigated by massive gas injections, error field modes have been seeded in a controlled way in dedicated experiments at JET [5]. By varying the toroidal phase of a superimposed $n=1$ magnetic perturbation field, the location of the mode locking could be influenced. The asymmetry of the radiated power measured by bolometers situated at two different toroidal locations was used to determine the toroidal peaking factor. It is important to note that the peaking of the heat flux to the first wall will deviate from the peaking of the radiation itself. However, quantifying the peaking of the radiation gives a more machine independent characterisation. For calculating the resulting temperature rise on in-vessel components, the heat flux distribution must be calculated from the radiation distribution using the realistic first wall geometry.

2. EXPERIMENTAL SET-UP

JET is equipped with four external coils, called EFCCs, which can be configured in a way to create an $n=1$ magnetic perturbation field (see Fig. 1). The toroidal angle of the main radial magnetic field vector can be varied on a shot-to-shot basis. The radiated power is measured by bolometers at two toroidal locations, 135° apart, one bolometer system consisting of mainly vertical channels, referred to as $P_{\text{rad,V}}$, the other one mainly horizontal channels, referred to as $P_{\text{rad,H}}$. Both bolometers view the plasma core and divertor. The total radiated power is calculated using different weights for each line-of-sight of the channel. The calculated powers

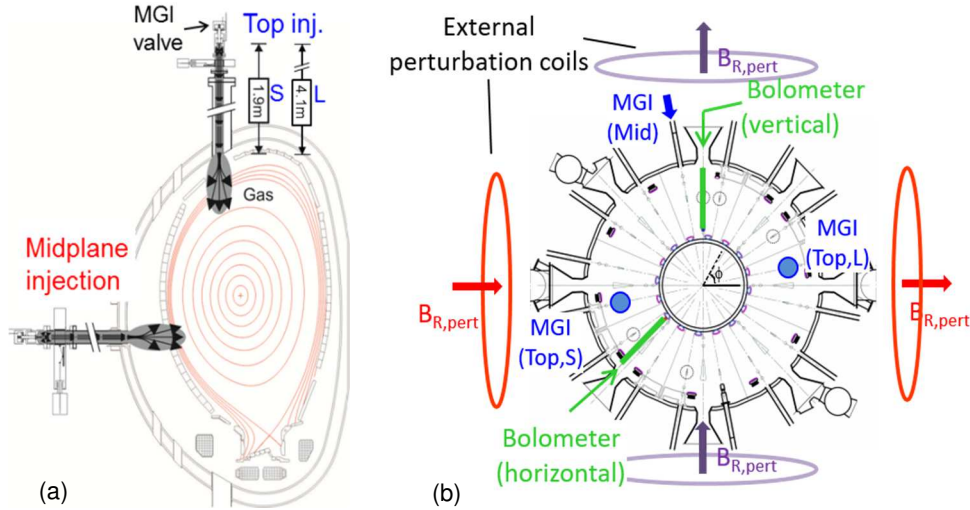


Fig 1: (a) Poloidal and (b) toroidal cross-section of the JET-tokamak showing the locations of the three massive gas injection valves and the horizontal ($P_{rad,H}$) and vertical ($P_{rad,V}$) bolometers. The red and purple circles indicate the toroidal location of the error field correction coils (EFCC). Note: the coils are not drawn to scale.

of the vertical and horizontal bolometers are in good agreement during the discharge phase prior to the disruption.

For disruption mitigation, JET uses three massive gas injection valves (MGI), of which two are located on top of the machine (“Top,S” and Top,L”) and one in the midplane (“Midpl”). Due to different distances to the plasma and different operating pressure, the amount of gas possible to inject varies for each of the valves. In particular the Top,L injector, being 4.1m away from the plasma compared to the Top,S injector having a distance of only 1.9m, has a 40% slower gas delivery. The valves can be operated individually or simultaneously, when a deliberate delay between the triggering time of two valves can be introduced to tailor the amount of gas delivered during the disruption by the respective valves. More details on the disruption mitigation system at JET can be found in [6].

Figure 2 shows a typical example of this experiment. During the flat top phase of an ohmic discharge as indicated by the plasma current, one coil pair has been energised to a level proven sufficient to impose an $n=1$ error field. The plasma density is slowly reduced until an $n=1$ mode arises and locks. A Real-Time algorithm is used to correct for the pickup of the vacuum magnetic perturbation field by determining the slope of the locked mode amplitude. At a predefined level, a trigger is issued to a MGIs. In the example shown here an injector from the top was used (Top,L).

The effect on the radiated power during the disruption is shown in more detail in Figure 3 (a)-(d). After some delay imposed by safety interlocks, the valve opens, which corresponds to the time when the MGI coil current peaks, and releases the gas. If not mentioned otherwise, a gas mixture of deuterium with 10% argon has been used. The gas arriving at the plasma is estimated using an Euler solution of a gas flow model as derived in [7]. The radiated power measured by the bolometer closest to the MGI ($\Delta\phi=88.5^\circ$) shows a sharp rise and reaches its maximum 2 millisecond before the radiation is becoming uniform as indicated by the bolometer measurements at $\Delta\phi=-146.5^\circ$. The power asymmetry factor defined as

$$\frac{\Delta P}{\Sigma P} = \frac{P_{rad,V}(\phi=90^\circ) - P_{rad,H}(\phi=225^\circ)}{P_{rad,V}(\phi=90^\circ) + P_{rad,H}(\phi=225^\circ)}, \quad (1)$$

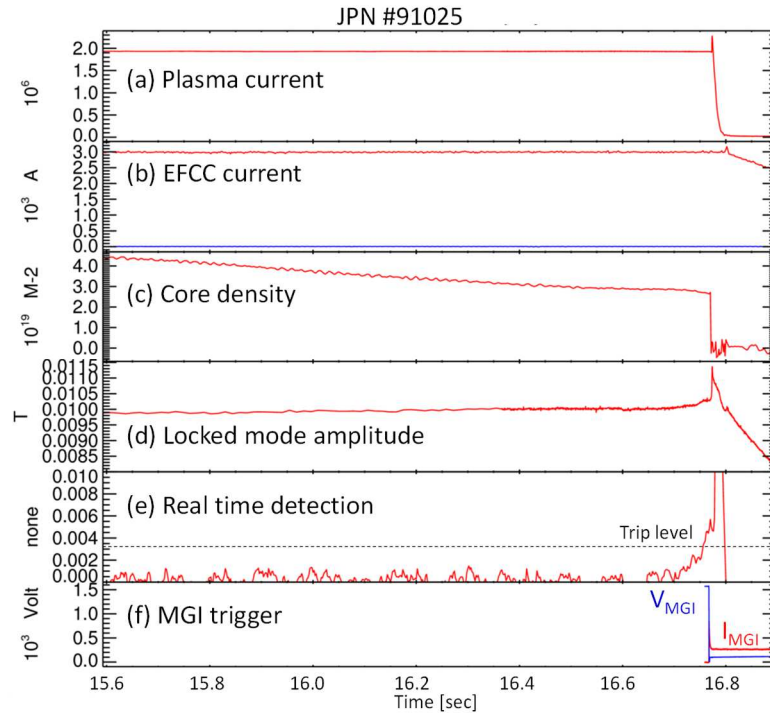


Fig 2: JET discharge with seeded error field mode: time traces of (a) plasma current, (b) EFCC currents corresponding to phase 0° , (c) line integrated plasma core density, (d) Amplitude of mode lock not corrected for magnetic perturbation field pickup, (e) real time detection of mode lock, (f) MGI power supply voltage and current.

reaches about 0.7 during the initial phase of the disruption. The toroidal position of the O-point of the $n=1$ mode at the outer mid-plane can be inferred from a set of saddle loops. In the discharge shown the O-point of the mode has been found at 46° , which is close to the injection location. Inverting the coil currents and hence the direction of the magnetic perturbation field, the resulting pattern of the radiated power is significantly different as shown in Figure 3(e): despite of the fast rise of the radiation at the location close to the massive gas injection location, uniformity is achieved in less than a millisecond. In this pulse the O-point was located at 226° and the gas has been injected mostly into the X-point of the mode. This illustrates the strong influence of the O-point position with respect to the location of the massive gas injection on the resulting radiation asymmetries. The experimental findings for single massive gas injections have been discussed in more details in [8]. A summary on disruption studies at JET in general is given in [9].

3. TOROIDAL RADIATION ASYMMETRIES FOR SINGLE AND DUAL INJECTIONS

The combination of the two EFCC coil pairs allows eight different phases forcing the developing $2/1$ mode to lock at the corresponding toroidal positions. Keeping all other plasma parameters, the same the power asymmetry factor can be determined as a function of the toroidal O-point position of the mode. Data from MGI induced disruptions without superimposed magnetic perturbation field already indicated a difference for the radiation asymmetry depending on the impurity gas used [8]. To investigate this further two sets of experiments were carried out, one with injection of a deuterium and 10% neon gas mixture and one with injection of the $D_2+10\%$ Ar gas mixture, both from the midplane. The results are summarised in figure 4, where the power asymmetry factor has been obtained for four discharge series: injection of the standard $D_2+10\%$ Ar from three different locations and one

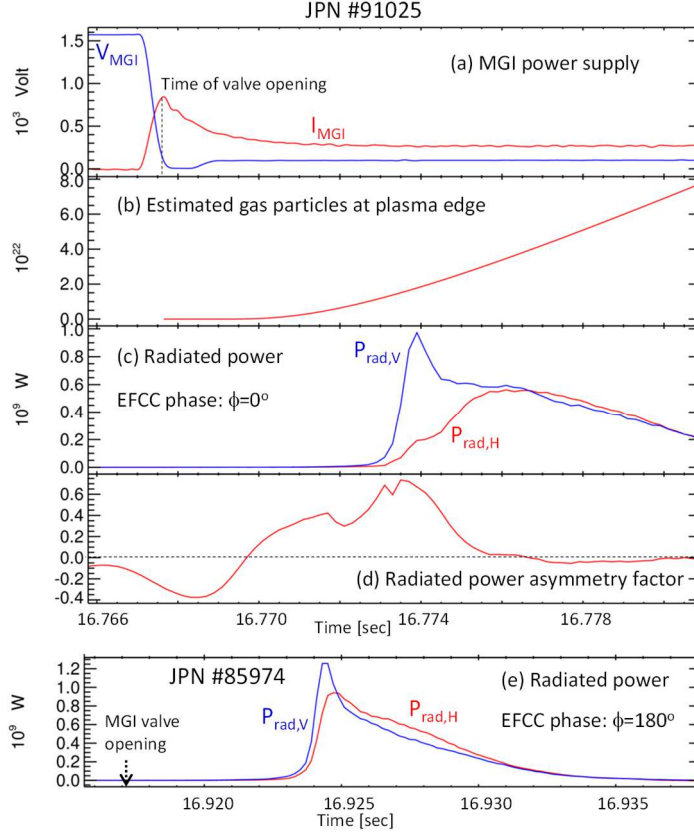


Fig 3: Time traces of the same discharge as in Fig 2: (a) response of the MGI power supply, (b) estimated amount of gas arriving at the plasma edge, (c) radiated power measured by the vertical (blue) and horizontal (red) bolometer and (d) the asymmetry factor of the radiated power. Box (e) shows the two measured radiated power for a pulse where the direction of the magnetic perturbation field has been inverted.

injection from the midplane using D2+10%Ne. It is worth noting that the longer the distance of the MGI from the plasma the larger is the variation of the power asymmetry. Also, the comparison of the two different impurity gas mixtures hints that the Argon gas mixture might have a larger toroidal peaking factor than the Neon gas mixture. The toroidal peaking factor TPF can be estimated by assuming a cosine-like radiation distribution $p_{dis}(\phi)$ driven by the $n=1$ mode [5] and a Gaussian-type toroidal distribution of the impurity density $n_i(\phi)$:

$$p_{dis}(\phi) = 1 + \Delta p \cos(\phi_{n=1} - \Delta\phi_{n=1} - \phi) \quad (2)$$

$$n_i(\phi) = n_{i,0} \exp(-(\phi - \phi_{inj})/\lambda_\phi^2) \quad (3)$$

with $\phi \in [-\pi, \pi]$ as toroidal coordinate and ϕ_{inj} as toroidal location of the MGI valve. The width of the impurity density distribution and the amplitude of the variation by the mode, λ_ϕ and Δp , as well as the phase offset $\Delta\phi_{n=1}$ are free parameters that can be used to fit the model to the measured power asymmetries. The total radiation measured at a specific toroidal location is then given by

$$P_{rad}(\phi) = \langle P_{rad}(\phi) \rangle p_{dis}(\phi) n_i(\phi) \quad (4)$$

and the toroidal peaking factor TPF for a given location of the O-phase of an $n=1$ mode, ϕ_m , as

$$TPF(\phi_m) = P_{rad,max}(\phi_m) / \langle P_{rad}(\phi_m) \rangle. \quad (5)$$

The expected TPF for the two injections from the midplane using deuterium argon and neon gas mixtures are depicted in figure 5. For injections with the MGI valve being toroidally close

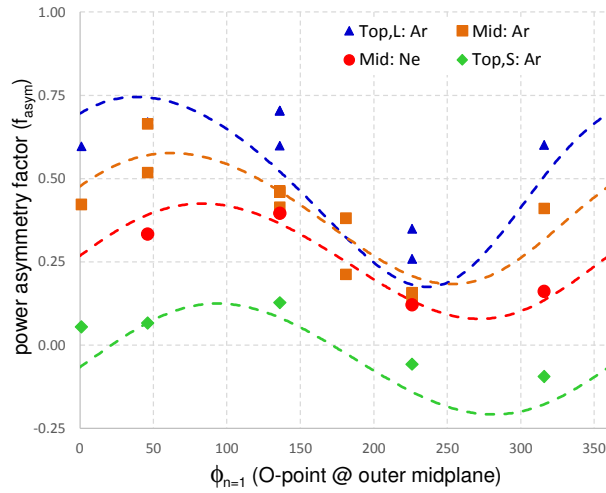


Fig. 4: Radiated power asymmetries for four set of scans: Top,L injection of D₂+10%Ar (blue), Midplane injection of D₂+10%Ar (orange) and of D₂+10%Ne (red) and Top,S injection of D₂+10%Ar (green). The dashed lines are estimated toroidal mode locking location dependency of the power asymmetry factor using Eq. (2). The free parameters [λ_ϕ , Δp , $\Delta\phi_{n=1}$] were for Top,S=[750°, 0.4, 30°], Mid(Ne)=[155°, 0.20, 20°], Mid(Ar)=[135°, 0.25, 0°] and Top,L=[110°, 0.4, -20°].

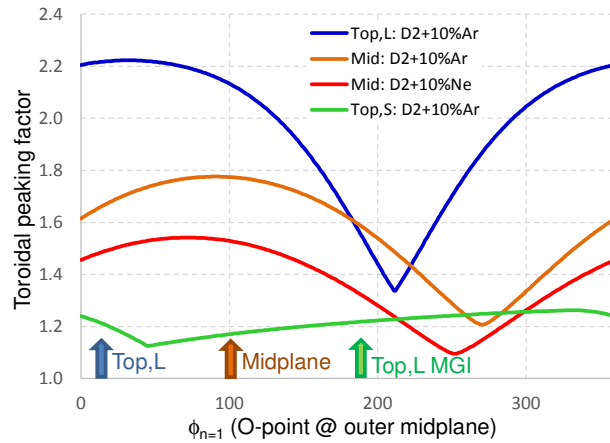


Fig. 5: Expected toroidal peaking factor for D₂+10%Ar (orange) and for D₂+10%Ne (red) from the midplane depending on the O-point position of a n=1 mode. The blue arrow indicates the toroidal location of the MGI.

to the O-point, the toroidal peaking factor is maximum due to the superposition of the radiation effect due to a localised injection and the n=1 asymmetry induced by the mode. In case of the Argon mixture the TPF can reach as much as 1.8 in contrary to the Neon mixture, where the TPF would not exceed 1.54.

For the four sets of experiments described above the following TPF ranges have been obtained:

	Top,L D ₂ +10%Ar	Midplane D ₂ +10%Ar	Midplane D ₂ +10%Ne	Top,S D ₂ +10%Ar
TPF min	~1.3	~1.2	~1.1	~1.1
TPF max	~2.2	~1.8	~1.5	~1.3

Table 1: Expected minimum and maximum toroidal peaking factors for the set of data shown in figure 4.

The lower TPFs for Neon and for the injection closest to the plasma (Top,S injector) are probably due to the faster gas delivery. It should be noted that for disruptions with higher thermal energy the Top,S injector has proven most efficient [8]. This is also indicated by a shorter current quench time for this series of pulses.

ITER will have the possibility to inject massive amount of impurities from several toroidal locations. It is expected that this will reduce the toroidal peaking factor provided the timing of the different injections is optimised. At JET only two injections from the same poloidal position, but two opposite toroidal locations are possible. Since the gas delivery of the two Top MGI valves is slightly different due to different orifices and gas delivery tube lengths, a careful timing scan for a dual injection using $D_2+10\%Ar$ gas mixture has been performed in this type of disruption scenario for a fixed chosen EFCC-phase causing the mode to lock at $\phi\sim 136^\circ$. The results are shown in figure 6, where the radiated power asymmetry factor has been plotted for different fractions of gas arriving from the Top,L MGI before the start of the current quench normalised to the to the sum of gas from Top,L and Top,S MGIs, i.e. $f_{inj}=ncq(\text{Top,L})/(ncq(\text{Top,L})+ncq(\text{Top,S}))$. The variable ncq corresponds to the amount of gas arriving at the plasma edge up to the start of the current quench inferred from the spike in the plasma current signal. The gas flow was estimated as described in [7]. The data show a clear monotonic increase starting from the Top,S only case ($f_{inj}=0$) up to the Top,L only case ($f_{inj}=1$). At $f_{inj}\sim 0.2$ the data deviate from this trend. Despite the fact that these results are well reproducible, the reason for this deviation is still under investigation. The tendency of the power asymmetry factor to increase with more dominant Top,L MGI, can be described with a simple model by estimating the impurity density as

$$n_i(\phi) = n_{i0} [f_{inj} \exp(-(\phi - \phi_{inj,1})/\lambda_\phi^2) + (1 - f_{inj}) \exp(-(\phi - \phi_{inj,2})/\lambda_\phi^2)] . \quad (6)$$

Using Eq. (2) and (3) and calculating the radiated powers at each of the locations of the horizontal and vertical bolometer the orange curve in figure 6 is obtained, which is in

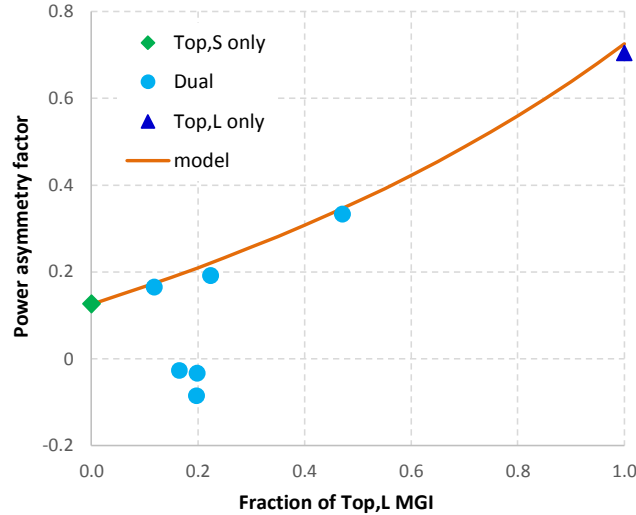


Fig. 6: Scan of radiated power asymmetry for dual injection. $f_{inj}=1$ corresponds to a single injection from of the Top,L MGI and $f_{inj}=0$ to a single injection of the Top,S MGI. The programmed delay for the dual injections was varied between -1 ms and +4 ms. The EFCC phase was the same in all pulses causing the mode to lock at $\phi=136^\circ$. The orange line represents the expected radiated power asymmetry for injections with different fractions of gas injected from the Top,L MGI. The free parameters of the model were determined as $\lambda_\phi=100^\circ$, $\Delta p=0.5$, $\Delta\phi_{h=1}=45^\circ$.

good agreement with the experimental data besides the data for $f_{inj} \sim 0.2$. One should note that the optimum settings to minimise the toroidal peaking factor will depend on the location of the O-point of the $n=1$ mode. However, the range in which the TPF will vary depending on the toroidal $n=1$ mode phase will be smaller for dual injections.

4. SUMMARY

The toroidal peaking factors for single injection from different locations and gas delivery characteristics have been determined. The smallest toroidal peaking factors have been found for the massive gas injection valve being closest to the plasma. Using an interpretative model, the TPF for this MGI was estimated to be in the range 1.1 to 1.3. This is likely due to shorter gas delivery tube of this MGI. As a result more gas will have arrived at the start of the thermal quench leading to a faster spread of the impurities and faster rise of the radiation. Gas mixtures using lower- Z impurity gases also tend to reduce the TPF. The change in the radiated power asymmetry with varying MGI gas fraction injected from two locations toroidally opposite could be described by a simple model combining the impurity density arising from the two simultaneous injections. In a very small window, in which the relative timing between the two injections was varied in the range of a few millisecond the power asymmetry reversed sign. Whether this is caused by the injection location having an impact on the mode phase, which might be more random for balanced simultaneous injections or whether the mode indeed locked to the external error field is still under investigation. In the coming campaign at JET, a Shattered Pellet Injection system will be operational. Studies in a similar scenario as presented here will be carried out to investigate the impact on the radiation asymmetry as a result from potential deeper penetration into the plasma core and higher core radiation.

ACKNOWLEDGEMENTS

This work has been carried out within the framework of the EUROfusion Consortium and has received funding from the Euratom research and training programme 2014-2018 under grant agreement No 633053. The views and opinions expressed herein do not necessarily reflect those of the European Commission or the ITER Organization.

REFERENCES

- [1] M. Lehnen *et al.*, Disruptions in ITER and strategies for their control and mitigation, *Journal Nuclear Material* **463** (2015), 39.
- [2] R.A. Pitts *et al.*, Final case for a stainless steel diagnostic first wall on ITER, *Journal Nuclear Material* **463** (2015), 748.
- [3] V.A. Izzo *et al.*, Impurity mixing and radiation asymmetry in massive gas injection simulations of DIII-D, *Physics of Plasma* **20** (2013), 056107.
- [4] N.W. Eidietis *et al.*, Poloidal radiation asymmetries during disruption mitigation by massive gas injection on the DIII-D tokamak, *Physics of Plasma* **24** (2017), 102504.
- [5] M. Lehnen *et al.*, Radiation asymmetries during the thermal quench of massive gas injection disruptions in JET, *Nuclear Fusion* **55** (2015), 123027.
- [6] U. Kruezi *et al.*, A new Disruption Mitigation System for deuterium-tritium operation at JET, *Fusion Engineering and Design* **96-97** (2015), 286.
- [7] S.A. Bozhakov *et al.*, Fuelling efficiency of massive gas injection in TEXTOR: mass scaling and importance of gas flow dynamics, *Nuclear Fusion* **51** (2011) 083033.
- [8] S. Jachmich *et al.*, Disruption mitigation at JET using massive gas injection, *Proceedings 43rd EPS conference on Plasma Physics, Europhysics Conference Abstracts*, **40A**, Leuven, Belgium (2016).
- [9] E. Joffrin *et al.*, *Proceedings 26th IAEA Fusion Energy Conference, Kyoto, Japan* (2016).